

Microscopic description of nuclear shape evolution from spherical to octupole-deformed shapes in relativistic mean-field theory

Jian-You Guo,* Peng Jiao, and Xiang-Zheng Fang

School of Physics and Material Science, Anhui University, Hefei 230039, People's Republic of China

(Received 10 January 2010; revised manuscript received 11 June 2010; published 7 October 2010)

Reflection asymmetric relativistic mean-field theory is used to investigate the shape evolution for even-even Th isotopes. The calculated deformations, matter density distributions, and potential energy surfaces demonstrate clearly the shape evolution from spherical to octupole deformed. Especially, it is shown that Th isotopes suffer two types of shape transition when the neutron number increases from $N = 126$ to $N = 156$. One is from spherical to octupole deformed around $N = 134$, and another is from octupole to quadrupole deformed around $N = 150$.

DOI: [10.1103/PhysRevC.82.047301](https://doi.org/10.1103/PhysRevC.82.047301)

PACS number(s): 21.60.Jz, 21.60.Ev, 21.60.Fw, 27.90.+b

The equilibrium shape of atomic nuclei as well as the transition between the different shapes has been the subject of a large number of theoretical and experimental studies (for a review, see, for example, Ref. [1] and references therein). Theoretical studies have typically been based on phenomenological geometric models of nuclear shapes and potentials [2], or algebraic models of nuclear structure [3], which have gained remarkable success in describing the phenomena of shape evolution and shape phase transition (SE/SPT) [4–6]. However, to provide greater detail, it is necessary to perform microscopic investigation of SE/SPT. In Ref. [7], the microscopic relativistic mean-field (RMF) theory is applied to Sm isotopes and the SE/SPT from spherical to axially deformed shapes is demonstrated clearly. In Ref. [8], a series of isotopes suggested as exhibiting critical-point symmetries are investigated by the microscopic approach. In combination with generator coordinate method (GCM), RMF theory has presented an excellent description of the general features of the transitions between spherical and axially deformed nuclei, the singular properties of excitation spectra, and the transition rates at the critical point of SPT [9]. In Ref. [10], the triaxial RMF theory is developed. In combination with GCM, the triaxial RMF theory has provided the deformation parameters to solve the five-dimensional collective Hamiltonian, which has presented a good description of the quantum phase transition between spherical and axially deformed shapes, as well as between spherical and triaxially deformed shapes [11–13]. Similar checks are performed for nuclear SE/SPT by using nonrelativistic microscopic approaches, including the self-consistent Skyrme-Hartree-Fock + BCS approximation, the Hartree-Fock-Bogoliubov approximation based on Gogny interaction, etc. The details can be found in the recent literature [14–17].

All these studies only relate to the phase transition between spherical and quadrupole shapes. However, in the Ra-Th region, it was observed that the nuclei ^{224}Ra and ^{224}Th , which have a very low-lying negative-parity band, soon merge with the positive-parity one for $J > 5$, which

implies that the octupole deformation should not be ignored in discussing the behavior of the phase transition [18,19]. In Refs. [20,21], the Bohr Hamiltonian with the collective coordinates involving quadrupole and octupole deformations has been introduced to describe the SE/SPT for Ra and Th isotopes, and ^{224}Ra and ^{224}Th are suggested to be the point of SPT from spherical to octupole-deformed shapes. Recently, an axial-symmetric reflection asymmetric relativistic mean-field (RAS-RMF) theory [22] has been developed. Its application to the shape evolution for Sm isotopes is presented in Ref. [23], where the shape/phase transition from U(5) to SU(3) symmetry is marked clearly with the possible octupole degree of freedom included. In this article, we examine the shape evolution from spherical to octupole-deformed shapes, and finally to quadrupole-deformed shapes, for Th isotopes by the microscopic approach.

The details of RAS-RMF theory can be found in Ref. [22]. To avoid repetition, in this brief report we do not repeat the related formalism. It is only noted that for axial-symmetric reflection-asymmetric systems, the RMF equations are solved by expanding the Dirac spinor in terms of the eigenfunctions of the two-center harmonic-oscillator (TCHO) potential [22]. For the nuclei studied in this article, the full $N = 17$ TCHO shells are taken into account and the convergence of the numerical calculations on the binding energy and the deformation has been checked (and has been found to be very good). The pairing correlations are considered by a constant gap approximation (BCS) with the pairing gap taken as $11.2 \text{ MeV}/A^{1/2}$ for even-number nucleons.

The binding energies coming from the RAS-RMF calculations with the newly improved effective interactions NL3 [24] (hereafter noted as NL3*) and PK1 [25] are respectively exhibited in Figs. 1(a) and 1(b) for Th isotopes, in comparison with the usual reflection symmetric RMF (RS-RMF) calculations and the available data [26,27]. From Fig. 1(a), it is seen that the binding energies from the RAS-RMF calculations are consistent with those from the RS-RMF calculations and comparable with the experimental data [26], especially for the neutron-rich side. The largest deviation between experimental and calculated data appears in ^{216}Th , which is less than 0.046 MeV. For $^{230-238}\text{Th}$, the binding energies from the RAS-RMF calculations agree with the data

* jianyou@ahu.edu.cn

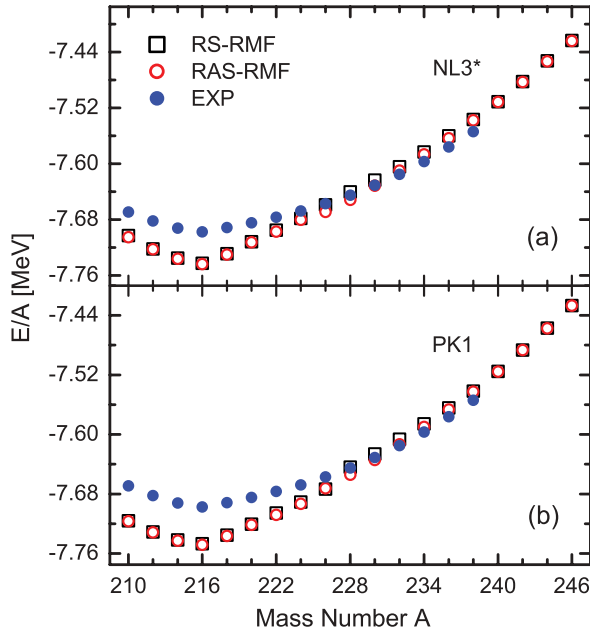


FIG. 1. (Color online) Binding energy per nucleon, E/A , for Th isotopes as functions of mass number A obtained from the RAS-RMF calculations (open circles) and the RS-RMF calculations (open boxes) in comparison with the data (solid circles).

better than those from the RS-RMF calculations. For $^{226,228}\text{Th}$, the RAS-RMF calculations increase the deviations between theory and experiment, which may originate from the binding energies underestimated in the usual RMF calculations. For $^{210-224}\text{Th}$, the RAS-RMF calculations agree with the RS-RMF calculations, which implies that the effect of octupole in these nuclei is negligible for the ground state. Similar conclusions are obtained with PK1 in the RAS-RMF calculations, as shown in Fig. 1(b). Compared with NL3, PK1 increases the binding of nucleons and improves the calculated data for $^{230-238}\text{Th}$, which are comparable to those from RAS. However, the RMF calculations with PK1 increase the binding energies for all the Th isotopes, which enlarges the deviations between theory and experiment for the nuclei with mass number below $A = 224$, whereas RAS increases the binding energies only for the nuclei holding octupole deformation as seen in Fig. 2(b). From this point, the agreement with experiment for binding energies should be due to the RAS approach.

In Figs. 2(a), 2(b), and 2(c), we display quadrupole deformation β_2 , octupole deformation β_3 , and hexadecupole deformation β_4 as the functions of mass number A for Th isotopes, respectively. From Fig. 2(a), we can see that the tendency for the change of shape with mass number is correctly reproduced in the RAS-RMF calculations and also in the RS-RMF calculations except for ^{226}Th . For ^{226}Th , the RS-RMF calculations fail to reproduce the experimental data [27], while the RAS-RMF calculations present a consistent result with experiment, which originates from the consideration of octupole degree of freedom. For the nuclei with mass number below $A = 226$, the axial-quadrupole deformation β_2 obtained in the RAS-RMF calculations is fully consistent with that obtained in the RS-RMF calculations.

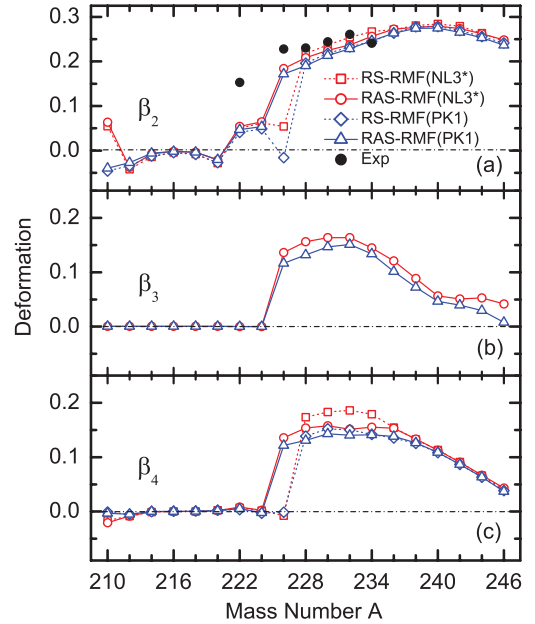


FIG. 2. (Color online) Quadrupole deformation β_2 , octupole deformation β_3 , and hexadecupole deformation β_4 for Th isotopes as functions of mass number A obtained from the RAS-RMF calculations and the RS-RMF calculations in comparison with the available data.

Similar to the case of quadrupole deformation, the octupole deformation from the RAS-RMF calculations with NL3* and PK1 is consistent. For the nuclei with mass number below $A = 226$, the octupole deformation is nearly zero. This is the reason why the binding energies and quadrupole deformation for these isotopes are almost the same with the RAS- or RS-RMF calculations. There exists obvious octupole deformation for nuclei from $A = 226$ to $A = 238$. Starting from $A = 232$, the octupole deformation decreases with the increasing of mass number, until $A = 246$, at which point the calculated octupole deformation is nearly zero again.

From Fig. 2(c), we find that the deformation β_4 obtained in the RAS-RMF calculations is similar to that obtained in the RS-RMF calculations for Th isotopes with the exception of ^{226}Th . ^{226}Th shows a clear hexadecupole deformation in the RAS-RMF calculations, which is different from that of the RS-RMF calculations.

These indicate, for deformations (β_2, β_4), the effect of the interactions, NL3* versus PK1, is comparable to that due to RS versus RAS in Th isotopes except for ^{226}Th . Therefore, it is difficult to judge whether the improvement in the data is due to the interactions or to the RAS approach. But, if the octupole deformation is observed, the effect of RAS can be checked. The conclusion derived from the binding energies can be tested from the deformation.

It is interesting to examine the shape evolution from spherical to octupole-deformed shapes, and finally to quadrupole-deformed shapes, by the microscopic theory.

To clarify the shape evolution, the matter density distributions of the ground states of Th isotopes versus z and y on the $x = 0$ plane are plotted in Fig. 3. It is clearly shown that $^{216-220}\text{Th}$ are spherical, and ^{222}Th is near spherical

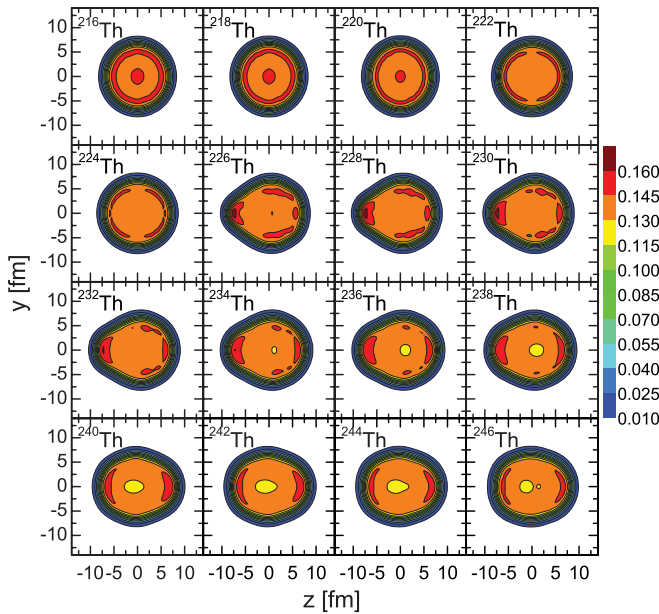


FIG. 3. (Color online) Matter density distributions of the ground states of Th isotopes versus z and y on the $x = 0$ plane, which were obtained from the RAS-RMF calculations with NL3*.

with a little quadrupole deformation, $^{226-232}\text{Th}$ are well-deformed nuclei with clear octupole shape, whereas ^{224}Th is a transitional nucleus from spherical to well-formed octupole shape. Starting from ^{232}Th , with increasing neutron number, the octupole deformation gradually decreases, the shape of Th isotopes develops toward the axial-symmetric reflection symmetry. As shown in Fig. 3, a pear-shape matter density distribution gradually evolves into a symmetrical ellipse shape. Particularly for $^{242-246}\text{Th}$, the reflection-asymmetric deformation almost disappears, the matter density distribution emerges itself from the axial-symmetric reflection symmetric shape, while ^{240}Th is a transitional nucleus from the reflection asymmetric deformation to the reflection symmetric deformation.

Furthermore, the contour plots of the total potential energies as functions of β_2 and β_3 for Th are shown in Fig. 4, where to save space only half of isotopes in $^{216-246}\text{Th}$ are plotted. Such contour plots have up-down symmetry in the (β_2, β_3) plane because of the equivalence between the states with positive and negative β_3 .

It is shown in Fig. 4 that the ground state of ^{218}Th is typically spherical, and that of ^{230}Th is typically octupole deformed with substantial quadrupole and octupole deformations, while in between the isotopes $^{222-226}\text{Th}$ mark a transition process from a sphere to an octupole-deformed shape. In detail, for ^{218}Th , with $N = 128$ close to the magic number 126, the ground state is clearly spherical. For ^{222}Th , although its ground state is still near spherical $(\beta_2, \beta_3) \sim (0.07, 0.00)$, an octupole minimum $(\beta_2, \beta_3) \sim (0.15, 0.10)$ is developed, which is about 0.99 MeV higher than the ground state. For ^{226}Th , the global minimum moves to $(\beta_2, \beta_3) \sim (0.19, 0.14)$, which has substantial quadrupole and octupole deformations and is only 1.84 MeV deeper than the nearly spherical minimum at $(\beta_2, \beta_3) \sim (0.05, 0)$. For ^{230}Th , the potential energy surface (PES)

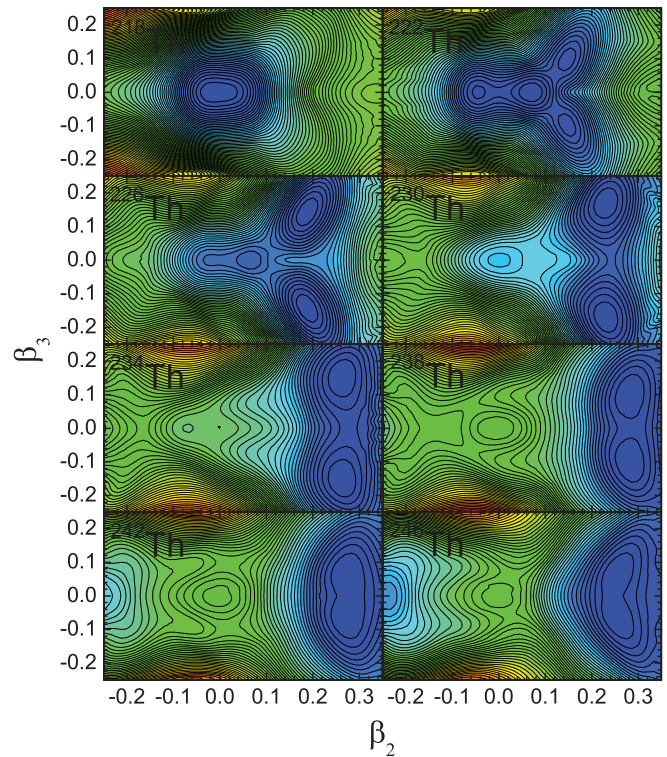


FIG. 4. (Color online) The potential energy surfaces of Th isotopes versus the quadrupole deformation parameter β_2 and the octupole deformation parameter β_3 obtained from the RAS-RMF calculations with NL3*.

around the octupolar global minimum becomes stiffer with a higher barrier against the nearly spherical minimum and the corresponding quadrupole-only state. Therefore, both ^{222}Th and ^{226}Th (also ^{224}Th not presented in Fig. 4) present an example of shape coexistence of near spherical and octupole deformation and also mark a shape transition from the spherical case ($^{216,218}\text{Th}$) to the octupole-deformed case (^{230}Th).

The ground states of Th isotopes will again become reflection symmetric with $\beta_3 \sim 0$ with the increase of the neutron number N , as can be seen from Fig. 2. From ^{230}Th to ^{238}Th , the global minima in PES are all octupole deformed, while the barrier from the octupole-deformed minima to the corresponding quadrupole-deformed states becomes lower with the neutron number N . For $^{242,246}\text{Th}$, the ground states become well quadrupole deformed with $\beta_3 \sim 0$, which is localized in the β_2 direction, but in the β_3 direction the potential surface is soft over a sizable interval. The shape evolution (with octupole softness) is thus presented in Th isotopes from $A = 230$ to $A = 246$.

Similar PESs have also been obtained with other parameter sets such as PK1 [25]. We also note that these results presented in Fig. 4 are consistent with the conclusions from Figs. 2 and 3, where only the information of deformations and matter density distributions for ground states are given.

In summary, a newly developed RAS-RMF theory is used to investigate the SE/SPT for even-even Th isotopes. It is shown that the RAS-RMF theory represents a satisfactory description

of the ground-state properties of atomic nuclei, including the binding energies and deformations. The RAS-RMF presents data on deformations, matter density distributions, and potential energy surfaces versus quadrupole deformation parameter β_2 and octupole deformation parameter β_3 , which show clearly the shape evolution from spherical to octupole deformed, and finally to quadrupole deformed. Particularly, it is shown that Th isotopes suffer two types of shape transition when the neutron number increases from $N = 126$ to $N = 156$, namely, from spherical to octupole deformed around $N = 134$ and from octupole to quadrupole deformed around $N = 150$.

We are very grateful to Dr. S. Q. Zhang and W. Zhang for their constructive comments and suggestions. Professor J. Meng is acknowledged for providing the code. This work was partly supported by the National Natural Science Foundation of China under Grant No. 10675001, the Program for New Century Excellent Talents at the University of China under Grant No. NCET-05-0558, the Program for Excellent Talents at Anhui Province University under Grant No. 2007Z018, the Education Committee Foundation of Anhui Province under Grant No. KJ2009A129, and the 211 Project of Anhui University.

-
- [1] J. L. Wood, K. Heyde, W. Nazarewicz, M. Huyse, and P. Van Duppen, *Phys. Rep.* **215**, 101 (1992).
- [2] A. Bohr, *Mat. Fys. Medd. K. Dan. Vidensk. Selsk.* **26**, 14 (1952).
- [3] F. Iachello and A. Arima, *The Interacting Boson Model* (Cambridge University Press, Cambridge, UK, 1987).
- [4] R. F. Casten and E. A. McCutchan, *J. Phys. G: Nucl. Part. Phys.* **34**, R285 (2007).
- [5] R. F. Casten, *Prog. Part. Nucl. Phys.* **62**, 183 (2009).
- [6] P. Cejnar and J. Jolie, *Prog. Part. Nucl. Phys.* **62**, 210 (2009).
- [7] J. Meng, W. Zhang, S. G. Zhou, H. Toki, and L. S. Geng, *Eur. Phys. J. A* **25**, 23 (2005).
- [8] R. Fossion, D. Bonatsos, and G. A. Lalazissis, *Phys. Rev. C* **73**, 044310 (2006).
- [9] T. Nikšić, D. Vretenar, G. A. Lalazissis, and P. Ring, *Phys. Rev. Lett.* **99**, 092502 (2007).
- [10] J. Meng, J. Peng, S. Q. Zhang, and S. G. Zhou, *Phys. Rev. C* **73**, 037303 (2006).
- [11] T. Nikšić, Z. P. Li, D. Vretenar, L. Próchniak, J. Meng, and P. Ring, *Phys. Rev. C* **79**, 034303 (2009).
- [12] Z. P. Li, T. Nikšić, D. Vretenar, J. Meng, G. A. Lalazissis, and P. Ring, *Phys. Rev. C* **79**, 054301 (2009).
- [13] Z. P. Li, T. Nikšić, D. Vretenar, and J. Meng, *Phys. Rev. C* **80**, 061301 (2009).
- [14] R. Rodríguez-Guzmán and P. Sarriguren, *Phys. Rev. C* **76**, 064303 (2007).
- [15] P. Sarriguren, R. Rodríguez-Guzmán, and L. M. Robledo, *Phys. Rev. C* **77**, 064322 (2008).
- [16] L. M. Robledo, R. R. Rodríguez-Guzmán, and P. Sarriguren, *Phys. Rev. C* **78**, 034314 (2008).
- [17] T. R. Rodríguez and J. L. Egido, *Phys. Lett. B* **663**, 49 (2008).
- [18] P. G. Bizzeti, in *Symmetries in Physics*, edited by A. Vitturi and R. Casten (World Scientific, Singapore, 2003), p. 262.
- [19] P. G. Bizzeti and A. M. Bizzeti-Sona, in *Nuclear Theory 24*, edited by S. Dimitrova (Heron Press, Sofia, 2005), p. 311.
- [20] P. G. Bizzeti and A. M. Bizzeti-Sona, *Phys. Rev. C* **70**, 064319 (2004).
- [21] P. G. Bizzeti and A. M. Bizzeti-Sona, *Phys. Rev. C* **77**, 024320 (2008).
- [22] L. S. Geng, J. Meng, and H. Toki, *Chin. Phys. Lett.* **24**, 1865 (2007).
- [23] W. Zhang, Z. P. Li, S. Q. Zhang, and J. Meng, *Phys. Rev. C* **81**, 034302 (2010).
- [24] G. A. Lalazissis, S. Karatzikos, R. Fossion, D. Pena Arteaga, A. V. Afanasjev, and P. Ring, *Phys. Lett. B* **647**, 111 (2007).
- [25] W. Long, J. Meng, N. Van Giai, and S. G. Zhou, *Phys. Rev. C* **69**, 034319 (2004).
- [26] G. Audi, A. H. Wapstra, and C. Thibault, *Nucl. Phys. A* **729**, 337 (2003).
- [27] S. Raman, C. W. Nestor Jr., and P. Tikkanen, *At. Data Nucl. Data Tables* **78**, 1 (2001).